

An Energy-limited Model of Algal Biofuel Production: Toward the Next Generation of Advanced Biofuels

Eric H. Dunlop and A. Kimi Coaldrake
Pan Pacific Technologies, Adelaide, SA 5075, Australia

Cory S. Silva and Warren D. Seider
Dept. of Chemical and Biomolecular Engineering, University of Pennsylvania, Philadelphia, PA 19104

DOI 10.1002/aic.14251

Published online October 22, 2013 in Wiley Online Library (wileyonlinelibrary.com)

Algal biofuels are increasingly important as a source of renewable energy. The absence of reliable thermodynamic and other property data, and the large amount of kinetic data that would normally be required have created a major barrier to simulation. Additionally, the absence of a generally accepted flow sheet for biofuel production means that detailed simulation of the wrong approach is a real possibility. This model of algal biofuel production estimates the necessary data and places it into a heuristic model using a commercial simulator that back-calculates the process structure required. Furthermore, complex kinetics can be obviated for now by putting the simulator into energy limitation and forcing it to solve for the missing design variables, such as bioreactor surface area, productivity, and oil content. The model does not attempt to prescribe a particular approach but provides a guide toward a sound engineering approach to this challenging and important problem. © 2013 American Institute of Chemical Engineers AICHE J, 59: 4641–4654, 2013

Keywords: biochemical engineering, simulation, process

Introduction

While humans have used algae as a food source for centuries,¹ the most recent history of algae as a biofuel dates back to the time of the Second World War. In 1941, Japan instituted an algal process for the production of diesel fuel to compensate for the major fuel shortages of the period.^{2–4} Germany did likewise but with an additional emphasis on fats.⁵ A short resurgence of interest in the potential for algal biofuels occurred in the United States in the 1950s,⁶ but it was only in the period of oil shocks during the 1970s and early 1980s that attention once again turned toward investigating its potential. The current interest in algal biofuels is probably best traced to the Aquatic Species Program at the Solar Energy Research Institute (now National Renewable Energy Laboratory) funded by the U.S. Department of Energy.^{7,8} One of its guiding principles was that no new fuel should interfere with or compete with the food chain. As carbon dioxide, some sunlight, and a little water, are the key building blocks for fuel production using algae, there was no potential for interference with the food chain and so the program focused on its further development.

Experimental and theoretical studies relating to the biology, cultivation, and harvesting, of algae for biofuels are now part of the research and development of many academic institutions and national laboratories in the United States and worldwide. By comparison, industry and other technology

development organizations have often focused at the level of unit operation or on a single production process appropriate to their immediate business objectives. More recently, in a concerted move toward the commercial-scale production of algal biofuels, the U.S. Department of Energy has funded a number of new initiatives, the framework for which was, in part, set in 2010 by its National Algal Biofuels Technology Roadmap.⁹ It noted that there was a need for an integrated systems model that included detailed engineering design and process modeling. The National Academy of Sciences¹⁰ has also issued a report outlining the challenges that lie ahead for algal oil production in the United States. The lack of an exhaustive properties database for biological materials has severely hampered attempts to develop models of algal growth and oil production. Similarly, the absence of reliable thermodynamics and kinetic rate constants has been problematic.^{11–13} Thus, any model of algal biofuels using computer-aided process design must overcome these limitations.

In spite of these difficulties, a number of models have been developed to address these¹⁴ and other issues, in particular economic modeling,^{15–19} and modeling concerned with the issue of maximum theoretical yields.²⁰ The use of such computer-aided models, however, needs to reflect a new era of integrated design optimization in which modeling is not limited to simulation and engineering analysis, but can be used to provide improved insights into the process systems engineering and drive innovation. The work presented in this article introduces an energy-limited model of algal biofuel production using the aspenONE® V7.3 software suite, with

Correspondence concerning this article should be addressed to E. H. Dunlop at edunlop@panpacific.com.au.

emphasis on Aspen Plus[®] 7.3.²¹ It takes an integrated system approach that offers solutions to some of the intractable problems in simulating light-driven biological processes in the chemical engineering design environment. The basic assumptions of the model and its physical properties needed for process design are established. Thermodynamic properties, particularly enthalpy and free energy, are identified. The process model is introduced and novel features explained. The construction of the flow sheet is then discussed in terms of key issues for modeling of an algal biofuels process. The concept of energy-limited algal growth and its implications for reactor design are then considered. It was found that the application of this concept obviates the need for detailed chemical kinetics schemes which are, at best, marginally useful. Significantly, it sets the upper limit for conversion efficiency and energetics. Selected results relating to the mass and energy balances obtained from the modeling are then examined, particularly with respect to water use, carbon flow, and lost work, demonstrating how the energy-limited model offers significant advantages, not only in terms of process design but also for meeting the criteria for the commercial-scale production of advanced algal biofuels.

Analysis envelope

This analysis concentrates on the energy/light-driven synthesis of triglycerides, which are converted to biodiesel through transesterification. The source of carbon dioxide is not important in this analysis, although a cement works source was used, as the authors had initially setup the model to study such a case in Queensland, Australia. Likewise, while the details of the transesterification process are important, and are the subject of numerous studies,^{22–26} in this study, an elementary model (not using detailed chemical kinetics) is sufficient. Note that other lipid conversion processes (e.g., hydro-treating to produce green diesel) could have been substituted for the biodiesel process in this model—and a similar analysis would have been carried out.

The overall envelope for this analysis has inputs: sea water, flue gas containing carbon dioxide, urea as a nitrogen source, and sodium hydroxide as a carbon dioxide absorber and outputs: biodiesel (methyl oleate), evaporated water, and blowdown from the reactors. The model takes as fixed 10^5 tonne/year of carbon dioxide, an average solar input of 5.7 kWh/(m²day), an average evaporation rate of 3.5 m³/(hc-h), and a photosynthetic efficiency of 4%. Variables not fixed, but which arise in the model, include pond size, cell concentration in the ponds, cell growth rate, oil content of the cells, and the number of times the cells divide (generation number). After running Aspen Plus to solve the model equations, it remains to select the endogenous metabolism extent and pond depth. Stated differently, the model is limited in that it focuses on the energetics of the reaction ponds and a hypothetical steady state using annual averages, although the authors are developing a dynamic model using Aspen Dynamics.

Development of the Key Components for a Model of Algal Biofuel Production

Initial work began with the simplest model to enable key components to be established and the basic design concept to be constructed. For example, biodiesel was characterized as methyl oleate (C₁₉H₃₆O₂) and the algae empirical formulae set as C₅₀H₅₀O₃₀N₇ with no sulfur or phosphorus.

During the second phase of development, greater complexity in inputs was introduced. Biodiesel, for example, was now presented as nine triacyl-glyceride (TAG) and nine methyl esters, while the algae empirical formulae for *Nannochloropsis salina*, a common species used in algae biofuel studies, became CH_{1.80}O_{0.40}N_{0.083}S_{0.0017}P_{0.002}.

Identifying the key components

Many databases for engineering design simulation have been primarily developed for the petroleum and heavy chemical processing industries. Consequently, many physical properties of the compounds needed for process design involving algae are not in conventional databases, are obscure bioproducts which have been poorly characterized, or do not exist. The compounds needed for this simulation fell into five categories. First, compounds already in a database, such as methanol, CO₂, O₂, N₂, urea, NH₃, water, and methyl oleate (biodiesel). Second, compounds that can be substituted; in particular, “Soluble Carbon/Organics” (SOLC), which can be substituted with glucose. Third, compounds that do not exist and, thus, need to be “invented.” Algae itself falls into this category, as does algal debris, and the range of oil-bearing cells of variable composition. In this context, the term “debris” refers to spent cells that are recycled or sent for conversion into animal feed. For the purposes of this simulation, debris is assumed to have the same chemical formula as algae and the same energy if used for animal feed. If debris is recycled, the debris degradation needs to be acknowledged in some way, but no figures are currently available. As an assumption, debris is considered to have only 80% of the heat of combustion of algae and heats of formation are calculated on this basis.

The fourth category involves defining the Algal Oil (triacyl-glyceride or TAG). Algae naturally produce a range of TAGs; they are too numerous and unpredictable to be useful in models of this type. It is, however, necessary to have physical properties that are as accurate as can realistically be obtained. It was, therefore, decided to use C₁₈ carbon chains as the standard, and to use triolein as the reference TAG, as it is a component in the Aspen database. The choice of triolein as the TAG automatically leads to methyl oleate as the biodiesel produced.

Finally, compounds of convenience are required. They are identical to the base algae to which they are always subsequently converted in an energy-less reaction. Examples are the subspecies AlgNew (algae newly synthesized in the reaction operation; i.e., not recycled or otherwise reused), AlgDeb (algae regenerated from recycled debris or smashed/lysed cells), and AlgGly (algae synthesized from glycerol). These subspecies are identical to “Algae” in every respect and have the same formulae, enthalpy of formation, and physical properties. The distinction is purely for internal “book-keeping” purposes to track where parts of the total biomass came from and to where they disappeared. A final reaction operation converts all these subspecies into “Algae.” This is referred to as “normalization.” It can be ignored if desired but is internally useful during the early stages of model development.

Development of assumptions

One of the early difficulties in the modeling of algal biofuel production is deciding how to deal with the range of triglycerides made by algae. While more than 100 triglycerides

Table 1. Components and Their Properties for Stage One Analysis

	Formula	ΔH_f (kJ/mol)	ΔS_f (kJ/mol-K)	ΔG_f (kJ/mol)	MW
Algae	C ₅₀ H ₅₀ O ₃₀ N ₇	-2,949	-7.30	-773	1228.98
OC5	C ₆₈ H ₇₁ O ₃₉ N ₉	-3,939	-9.80	-1,016	1638.35
OC35	C ₅₈ H ₇₆ O ₂₄ N ₅	-2,982	-7.66	-697	1227.26
OC70	C ₅₅ H ₈₈ O ₁₃ N ₂	-2,424	-6.45	-500	985.31
TAG	C ₅₇ H ₁₀₄ O ₆	-2,202	-6.03	-404	885.45

are known, their physical properties are not usually available. In model development, this was approached in two stages. First, in Stage One, a single representative triglyceride, triolein, was chosen due to its properties being readily available. It forms methyl oleate to be used as biodiesel and its properties were also readily available. This greatly simplified the development of the model and allowed attention to be focused on key issues. Consequently, this model is used in subsequent discussions when focusing on broad principles rather than detailed engineering. For example, an algae empirical form was chosen that did not contain sulfur or phosphorous. While sulfur and phosphorous are very important biologically, they contribute only in a minor way to the mass and energy balances. Table 1 contains a summary of the properties assumed. Note the components OC5, OC35, and OC70 are defined shortly.

In Stage Two, these simplifications were removed and a real algae, *Nannochloropsis salina*, which has an empirical formula of CH_{1.80}O_{0.40}N_{0.083}S_{0.0017}P_{0.002}, was selected. A range of nine triglycerides were then established as important, because not all algae processing is directed to biofuels (Table 2). Some is geared toward pharmaceuticals, and higher numbered triglycerides in the C₆₃ to C₆₉ range are known to have medicinal applications.²⁷ They exist in smaller quantities but merit inclusion for the nonfuel applications of the model. The single TAG, triolein, is now replaced by the composite triglyceride TAG9, which refers to a weight-average composite of the nine triglycerides used. Once nine triglycerides are incorporated into the model, nine methyl esters automatically follow.

Another difficulty in developing an algal biofuels process model is the terminology, “algae,” with or without oils. All species of cells, including algae, need a baseline quantity of triglyceride oils for structure and function. Algae overaccumulate these oils, which is the basis for this process. Because it was not possible to obtain data that dealt reliably with this issue, an explicit objective of the model has been to remove as much ambiguity as possible. Thus, “algae” refers to cells that contain only the base level of oil with no extra-accumulation, while “oil-bearing cells” are defined as OC5, OC35, and OC70 containing, respectively, 5, 35, and 70 wt % of triglyceride oil. OC70, for example, was defined to have the arithmetic sum of 30 wt % of the heats of combustion of algae (19.44 MJ/kg) and 70 wt % of the TAG (39.66 MJ/kg). Cells of any arbitrary composition can be similarly defined by mixing molar quantities.

To reduce confusion and permit analysis of the process, the model is explicitly developed in two separate stages: the first reaction operation, in which cells grow without making oil, and the second reaction operation, in which there is no new cell growth, but oil accumulates. In actual operation, these two stages may occur in one reactor, but the benefits of two reaction operation models are becoming apparent.²⁸

Defining the thermodynamic properties of the key components

The heats of formation are fundamental to calculate the heats of reaction and are rarely known for biological substances. The latter can be used as a starting point to arrive at reasonable approximations for the enthalpy of combustion, but even these are often ambiguous. The best available data appear to be that of Larsson on Baker’s yeast (*Saccharomyces cerevisiae*),²⁹ who also provides entropy data. These were used to estimate the thermodynamic properties in Figure 1. Larsson’s data give 19.44 MJ/kg for the enthalpy of combustion, and -150 J/mol/K for the entropy, based on a molecular weight of 25.229. Our molecular weight is larger, at 1208.976. This allows a conversion of the Larsson data to -23,900 MJ/kmol for the enthalpy of combustion and -7.036 MJ/kmol/K for the entropy. It is clear that this area requires further, careful work for the future development of biofuels.

The enthalpy and free energy of formation of the required compounds were then calculated from the reverse of the combustion reaction with the equations for the formation of water, carbon dioxide, SO₂, and P₂O₅, summed according to the first law of thermodynamics. They are reported in later sections.

Identifying the main reactions and establishing their heats of reaction

Having obtained the required thermodynamic properties, some noninteger reaction stoichiometry is needed to provide the remaining information. To calculate the heats of reaction, the heats of formation of each compound are required from within the simulation database or the NIST database. Documenting the source of the data is helpful as conflicting data

Table 2. Components and Their Properties for Stage Two Analysis

Algae Empirical Formula: <i>Nannochloropsis salina</i> CH _{1.90} O _{0.40} N _{0.083} S _{0.0017} P _{0.002}				
Triglycerides (TAG)				
C ₄₅ H ₈₆ O ₆				Trimyristin
C ₅₁ H ₉₈ O ₆				Tripalmitin
C ₅₁ H ₉₂ O ₆				Tripalmitolein
C ₅₇ H ₁₁₀ O ₆				Tristearin
C ₅₇ H ₁₀₄ O ₆				Triolein
C ₅₇ H ₉₈ O ₆				Trilinolein
C ₆₃ H ₁₂₂ O ₆				Triarachine
C ₆₃ H ₉₂ O ₆				Tricosapentenate
C ₆₉ H ₁₂₈ O ₆				Trierucin
C _{63.830} H _{116.2086} O _{7.263}				TAG9
Methyl Esters				
C ₁₅ H ₃₀ O ₂	C14:0	Methyl myristate	2%	wt%
C ₁₇ H ₃₄ O ₂	C16:0	Methyl palmitate	36.5%	wt%
C ₁₇ H ₃₂ O ₂	C16:1	Methyl palmitoleate	37.5%	wt%
C ₁₉ H ₃₈ O ₂	C18:0	Methyl stearate	2%	wt%
C ₁₉ H ₃₆ O ₂	C18:1n9	Methyl oleate	9%	wt%
C ₁₉ H ₃₄ O ₂	C18:2n6	Methyl linoleate	3%	wt%
C ₂₁ H ₃₄ O ₂	C20:4n6	Methyl arachidonate	2%	wt%
C ₂₁ H ₃₂ O ₂	C20:5n3	Methyl eicosapentenate	7%	wt%
C ₂₃ H ₄₄ O ₂	C22:1	Methyl erucinate	1%	wt%
Oil Bearing Cells				
OC5		C _{47.1619} H _{89.3726} O _{17.9517} N _{3.6496} S _{0.0748} P _{0.0879}		
OC35		C _{52.4180} H _{97.9490} O _{14.5756} N _{2.4971} S _{0.0511} P _{0.0602}		
OC70		C _{58.5501} H _{107.9549} O _{10.6368} N _{1.1525} S _{0.02368} P _{0.0278}		

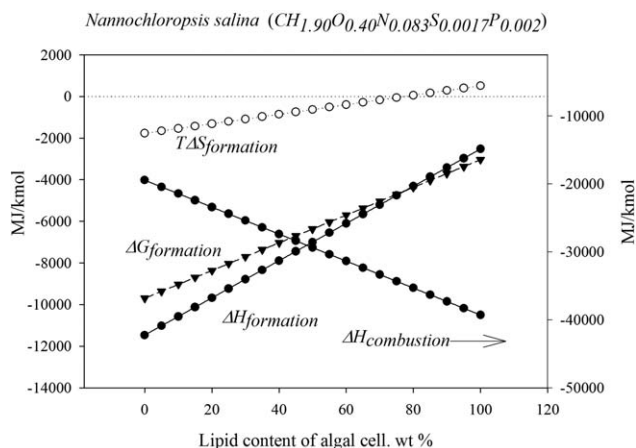


Figure 1. Thermodynamic properties of algal cells of varying oil concentration at 25°C.

occur occasionally. Thermodynamic data for some compounds are not available in these databases, either because the compounds are contrived in the modeling process, as in the case of algae or OC5 discussed above, or because their importance has only so recently been recognized that they have not yet been incorporated, as with, for example, some of the higher triglycerides.

In view of noninteger stoichiometric coefficients, balancing the equations can be difficult. To facilitate this process, a small matrix-based stoichiometry generator was developed. In the early stages of model development, when only carbon, hydrogen, oxygen, and nitrogen were used, a 4×4 matrix

was developed which, after inversion, yielded stoichiometric coefficients. When sulfur and phosphorous were added, a 6×6 matrix was created, but the matrix can be adjusted for any degree of complexity, as shown in Table 3. In this table, A is the atom matrix, with the rows and columns representing the atoms and the chemical components. The weight percents of C, H, and O are shown in the desired product, TAG9, vector. Then, the stoichiometric coefficients, a, b, \dots, f , in the reaction are in the X vector, which is computed by mass balance, $X = A^{-1}B$. The resulting reaction, in which negative stoichiometric coefficients denote reactants and positive ones denote products, is shown at the bottom of Table 3.

Clearly, it is impractical, and likely impossible, to analyze a reaction system having large numbers of chemical reactions involving thousands of chemical components. Instead, a set of overall (or lumped) reactions, which represent the conversion of CO_2 to algae and algae to triglycerides, are defined. The enthalpies and free energies of reaction are estimated as shown in Table 4 and tabulated for all reactions in Table 5. As mentioned previously, it is convenient to group reactions (1–3) that involve cell growth without oil generation into reaction operation 1; and reactions (6–11) that accumulate oil without new cell growth in reaction operation 2. Reactions 4 and 5 (equivalent to 12 and 13) represent the cell's "endogenous metabolism." In reaction 4 (12), algae break down to CO_2 , releasing energy for metabolism, whereas in reaction 5 (13), algae yield nonuseful "soluble carbon," which is modeled as glucose herein. Finally, the lysis reactions (14–16) break down the oil cells, releasing TAG and algae debris. These assumptions should be

Table 3. Calculations Using the Matrix Stoichiometry Generator

Example:
 $a \text{ OC70} + b \text{ Debris} + c \text{ O}_2 + d \text{ H}_2\text{O} + e \text{ SO}_4^{2-} + f \text{ HPO}_4^{2-} \rightarrow \text{TAG9}$

INPUT MATRIX $[A]$
 Raw materials

	OC70	Debris	O ₂	H ₂ O	SO ₄ ²⁻	HPO ₄ ²⁻
C	58.5501	1	0	0	0	0
H	107.955	1.9	0	2	0	1
O	10.6368	0.4	2	1	4	4
N	1.1525	0.083	0	0	0	0
S	0.02368	0.0017	0	0	1	0
P	0.02780	0.002	0	0	0	1
	a	b	c	d	e	f

RESULT VECTOR $[B]$
 Desired product

TAG9
63.83
116.21
7.263
0
0
0

INVERSE MATRIX $[A]^{-1}$

0.022389	1.51E-21	0	-0.269	0	3.5E-17
-0.31089	1.01E-17	0	15.793	0	-2.1E-15
0.399691	-0.25	0.5	-1.420	-2	-1.75
-0.91317	0.5	0	-0.432	0	-0.50
-1.7E-06	-3.8E-19	0	-0.020	1	4.3E-19
-6.5E-07	-1.6E-19	0	-0.024	0	1

SOLUTION VECTOR $[X]$
 Stoichiometric coefficients

1.429097	a OC70
-19.84379	b Debris
0.091596	c O ₂
-0.183107	d H ₂ O
-0.00011	e SO ₄ ²⁻
-4.13E-05	f HPO ₄ ²⁻

$[A][X] = [B]$ or $[X] = [A]^{-1}[B]$

A positive coefficient in the solution vector denotes a reactant, while a negative coefficient denotes a product.

Thus the balanced equation for this example is :-

$$1.429097 \text{ OC70} + 0.091596 \text{ O}_2 \rightarrow \text{TAG9} + 19.84379 \text{ Debris} + 0.183107 \text{ H}_2\text{O} + 0.00011 \text{ SO}_4^{2-} + 4.13\text{E-}05 \text{ HPO}_4^{2-}$$

Table 4. Example of Calculating Heats of Reaction for Each Reaction Operation

	Reactants						Products					
	<i>n</i>	<i>H_r</i> (kJ/mol)	<i>nH_r</i> (kJ/mol)	<i>S_r</i> (kJ/mol-K)	<i>TS_r</i> (kJ/mol)	<i>nG_r</i> (kJ/mol)	<i>n</i>	<i>H_p</i> (kJ/mol)	<i>nH_p</i> (kJ/mol)	<i>S_p</i> (kJ/mol-K)	<i>TS_p</i> (kJ/mol)	<i>nG_p</i> (kJ/mol)
Reaction 1												
						46.5 HCO ₃ ⁻ + 18 H ₂ O + 3.5 Urea						
CO ₂	46.5	-393.80	-18,312	0.003	1	-18,352	AlgNew	-2,949	-2,949	-7.30	-2,175	-774
Water	18	-286.01	-5,148	-0.163	-489	-4,273	O ₂	0	0.00	0.21	61.13	-2,583
Urea	3.5	-333.00	-1,165	-0.522	-156	-621	Sum Products	Endothermic	-2,949			-3,357
Sum Reactants			-24,626			-23,245	kJ/mol overall reaction	Unfavorable				
Heat of Reaction = ΣProducts - ΣReactants				ΔH	21,677	kJ/mol overall reaction						
				ΔG	19,889	kJ/mol overall reaction						
Reaction 6												
						Algae + 31.2 HCO ₃ ⁻ + 28.2 H ₂ O → 1.4 OC 35 + 43.5 O ₂ + 31.2 OH ⁻						
CO ₂	31.2	-394	-12,287	0.003	1	-12,313	OC35	-2,982	-4,175	-7.664	-2,284	-978
Algae	1	-2,949	-2,949	-8.758	-2610	-339	O ₂	0	0	61.135	18,218	-2,659
Water	28.2	-2,861	-8,065	-0.613	-49	-6,694	Sum Products	Endothermic	-4,175			-3,637
Sum Reactants			-23,301			-19,347	kJ/mol overall reaction	Unfavorable				
Heat of Reaction = ΣProducts - ΣReactants				ΔH	19,126	kJ/mol overall reaction						
				ΔG	15,710	kJ/mol overall reaction						

reasonable to estimate the energy requirements of the cultivation system.

Returning to the stoichiometric matrix in Table 3, for each reaction in Table 5, just two compounds are needed: (1) the reactant, usually HCO₃⁻ or algae and (2) the desired product, typically algae (reactions 1 and 2) or an oil-containing cell (reactions 6–11). The remaining compounds are those that appear in each reaction: CO₂, H₂O, O₂, N₂, and urea. The signs of the stoichiometric coefficients in the solution vector identify reactants (negative) and products (positive).

Modeling the Process of Algal Biofuel Production

The use of process simulators, and aspenOne in particular, for bioprocesses has been proposed in the past, but has met with difficulties.^{30,31} Since then, a number of Aspen Plus models have appeared for cellulosic ethanol^{31–33} and, more recently, for algal biofuels building on these and similar models,^{18,26} but each presupposes a process flow sheet.

This section presents a strategy for creating models when designing processes to cultivate algae, extract TAG, and convert TAG to biodiesel. Three levels of modeling are introduced briefly in the subsections below. The first, a heuristic model, has been used for techno-economic analyses in the early stages of process design and is demonstrated here.

1. Heuristic model (to be used in the Discovery mode): This is intended to permit the examination of process alternatives (real and imaginary) to discover the necessary components for a process to conform to the strict limitations of experimentally measured photosynthetic efficiencies, subject to conventional mass and energy balances. It is intended to provide maximum flexibility in design, permitting streams to be introduced as needed, recycled if necessary or desired, and generally used to identify the areas in which effective operation may occur. Overall reactions are modeled to provide sound estimates of the energy requirements, while yielding key estimates for capital cost estimation—especially the cultivation pond area, pipe lengths, and pump sizes. Note that equipment items, such as pipes and pumps, are included only when energy and installation costs are estimated to be significant.

2. Steady-state process model: Here, separate reaction operations in the discovery stage, principally for stoichiometric calculations of heats and free energies of reaction, are combined to model tubular or stirred-tank reactors using chemical kinetics equations with rate constants and rates of conversion. Also, missing unit operations are added to provide better estimates of operating and capital costs.

3. Time-dependent reactor model: To accurately represent the light intensity to grow algae, dynamic modeling of the sunlight intensity over 365 days of the year is needed, as sunlight is obviously not at steady state, either throughout the day or throughout the year. A dynamic model is under construction using Aspen Dynamics®. It is also possible to address the nonsteady-state nature of sunlight using the steady-state model over separate, discrete time intervals, an approach which, so far, has proven to be adequate to modeling needs.

Process block diagram

The process model was initiated with a generalized process block flow diagram (Figure 2), followed by a process simulation flow sheet. The construction of the simulation flow sheet involved setting up the Calculator Blocks in

Table 5. Reactions with Corresponding Heats of Reaction

Reaction Number		ΔH kJ/mol of reaction	ΔG kJ/mol of reaction
Reaction Operation 1			
1	$46.5 \text{ HCO}_3^- + 18 \text{ H}_2\text{O} + 3.5 \text{ Urea} \rightarrow \text{AlgNew} + 42.25 \text{ O}_2 + 46.5 \text{ OH}^-$	21,676	19,889
2	$3.5 \text{ Urea} + 15.5 \text{ Glycerol} + 12 \text{ O}_2 \rightarrow \text{AlgGly} + 44 \text{ H}_2\text{O}$	-3,888	-6,682
3	$\text{Debris} \rightarrow \text{AlgDeb}$	4,778	4,344
4	$\text{AlgNew} + 42.25 \text{ O}_2 \rightarrow 46.5 \text{ CO}_2 + 3.5 \text{ Urea} + 18 \text{ H}_2\text{O}$	-21,676	-21,264
5	$3 \text{ AlgNew} + 75 \text{ H}_2\text{O} \rightarrow 10.5 \text{ N}_2 + 7.5 \text{ O}_2 + 5 \text{ SOLC}$	-1,148	-3,600
Reaction Operation 2			
6	$\text{Algae} + 31.2 \text{ HCO}_3^- + 28.2 \text{ H}_2\text{O} \rightarrow 1.4 \text{ OC35} + 43.5 \text{ O}_2 + 31.2 \text{ OH}^-$	19,126	15,710
7	$142.5 \text{ HCO}_3^- + \text{Algae} + 129 \text{ H}_2\text{O} \rightarrow 3.5 \text{ OC70} + 199.25 \text{ O}_2 + 142.5 \text{ OH}^-$	24,993	19,042
8	$\text{Algae} + 10.4 \text{ Glycerol} \rightarrow 1.4 \text{ OC35} + 7.1 \text{ O}_2 + 13.4 \text{ H}_2\text{O}$	1,973	1,209
9	$\text{Algae} + 47.5 \text{ Glycerol} \rightarrow 3.5 \text{ OC70} + 33 \text{ O}_2 + 61 \text{ H}_2\text{O}$	9,132	5,487
10	$1.2857142857 \text{ Algae} + 3.7142857143 \text{ HCO}_3^- + 3.3571428571 \text{ H}_2\text{O} \rightarrow 1 \text{ OC5} + 5.1785714286 \text{ O}_2 + 3.7142857143 \text{ OH}^-$	2,276	1,740
11	$1.2857142857 \text{ Algae} + 1.238095238 \text{ Glycerol} \rightarrow 1 \text{ OC5} + 0.845238095 \text{ O}_2 + 1.595238095 \text{ H}_2\text{O}$	234	146
12	$\text{Algnew} + 42.25 \text{ O}_2 \rightarrow 46.5 \text{ CO}_2 + 3.5 \text{ Urea} + 18 \text{ H}_2\text{O}$ (duplicate of Reaction 4)	-21,676	-21,264
13	$3 \text{ Algnew} + 75 \text{ H}_2\text{O} \rightarrow 10.5 \text{ N}_2 + 7.5 \text{ O}_2 + 25 \text{ SOLC}$ (duplicate of Reaction 5)	-1,148	-3,600
Lysis Operation			
14	$\text{OC35} + 0.187970 \text{ H}_2\text{O} \rightarrow 0.714286 \text{ Debris} + 0.206767 \text{ O}_2 + 0.390977 \text{ TAG}$	-3,344	-3,083
15	$1.4 \text{ OC70} + 0.4 \text{ H}_2\text{O} \rightarrow 0.4 \text{ Debris} + 0.3 \text{ O}_2 + \text{TAG}$	-1,899	-1,768
16	$\text{OC5} + 0.031328 \text{ H}_2\text{O} \rightarrow 1.285714 \text{ Debris} + 0.31328 \text{ O}_2 + 0.065163 \text{ TAG}$	-6,131	-4,963

Aspen Plus that are required to solve for the unknowns, and to collect and analyze data. The unknowns include the physical construction of the reactor (i.e., surface area), and the modeling of solar energy and light limitation, evaporation, and CO₂ absorption. Including these variables in the simulation provides a more accurate picture of the expected algal growth.

There are several key process operations in Figure 2. First, a smokestack is modeled as a source of CO₂, and the CO₂ is absorbed in water, and not bubbled into the following two reaction operations. The first reaction operation models just algae growth, and a separate reaction operation models lipid production. Note that it was helpful to have these last three operations totally independent, although all three operations could be carried out in a single equipment item. At this stage of process development, the type of reactor is not specified; that is, raceways or glass tubes (e.g., photo-bioreactors). It was also deemed advisable to retain maximum flexibility in the modeling process by having recycle streams available to suit different design concepts. Water, biomass, and glycerol may or may not be recycled, according to different needs.³⁴ An additional possibility was created to bring in glycerol that has originated outside of the defined flow sheet, as the additional glycerol can be viewed as a supplemental carbon source. This may be helpful when there is an excess availability of glycerol from other processes. Also, bleed streams

are provided to purge inert species; for example, buildup of salt as evaporation occurs.

Construction of the process simulation flow sheet

When constructing the process simulation flow sheet, the following considerations are important. The absorber is modeled as rate-based, which is more accurate than equilibrium-staged, and allows the absorption rate constants to be adjusted to reflect mass-transfer performance. Also, accurate species diagrams are needed, as shown in Figure 3, not just for CO₂ and water but also for phosphate. These include the ionic species, especially the bicarbonate ion, as the industry returns to the higher pHs (9–10) used in food processing to control contamination.³⁵

Next, as mentioned above, the cultivation section is simulated using two reaction operations, one for algal cell generation and the other for lipid production. Both use information recycle loops, as illustrated in Figure 4, with blocks that account for solar energy input, that estimate the conversion of the limiting reactant, the extents of reactions, and the heats of the reactions, and that account for energy losses due to the evaporation of water.

Specifications for the model are measured local rates of evaporation, local solar inputs, pond depth, and photosynthetic efficiency (typically 4%). Incident light, in kW, is one of the most fundamental variables in this process, and setting

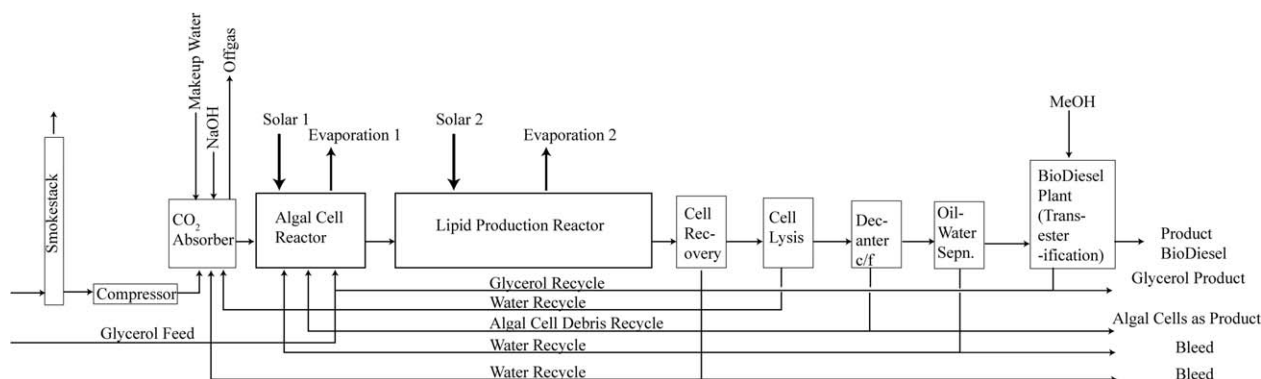


Figure 2. Generalized process block flow diagram.

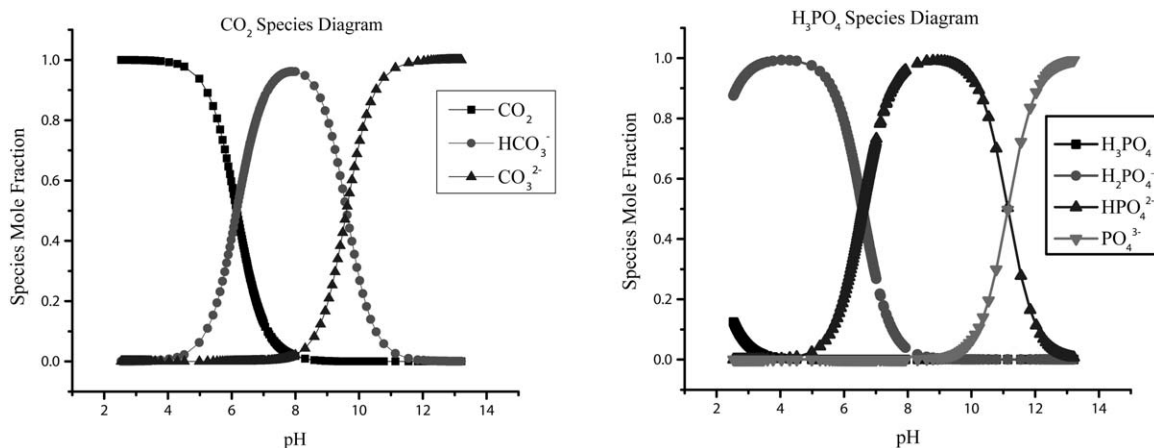


Figure 3. Species diagrams for the carbon dioxide and phosphate systems.

up the simulation flow sheet to run in light limitation is critical. Pond depth is typically ignored, yet it is of fundamental importance. Both of these factors are discussed in the subsection on Energy-Limited Algal Growth.

Returning to Figure 2, the block diagram shows the key information flows in the heuristic model for the entire process to grow and convert algae to biodiesel. As mentioned above, for the first reaction operation (algal cell generation), the information recycle loop in Figure 4 is used. Here, the material inputs are mixed with recycle stream, S8. The combined stream, S1, is sent to a single-stream heat exchanger (implemented using the HEATER block), E-100, where 100% of the solar energy flux (KW/m^2) multiplied by a guess for the cultivation area, A_1^* , is the heat duty added to S1. The effluent, S2, is sent to a RSTOIC block, R-100, that models reactions 1–5 in Table 5, and

algae biomass is produced until the limiting reagent (urea in this case) is entirely consumed. Meanwhile, the extents of the other reactions are estimated and stored in the Calculator block.

In the E-101 single-stream heat exchanger block, the extents of reaction are combined with the heats of reaction to determine the amount of energy consumed in biomass production. Also, the area for the next iteration is determined

$$A_1 = \frac{\sum_{i=1}^5 \xi_i \Delta H_{R_i}}{\Phi_s \phi} \quad (1)$$

where A_1 is the area for biomass generation, ξ_i is the extent of reaction i , ΔH_{R_i} is heat of reaction i , Φ_s is solar energy flux, and ϕ is the photosynthetic efficiency.

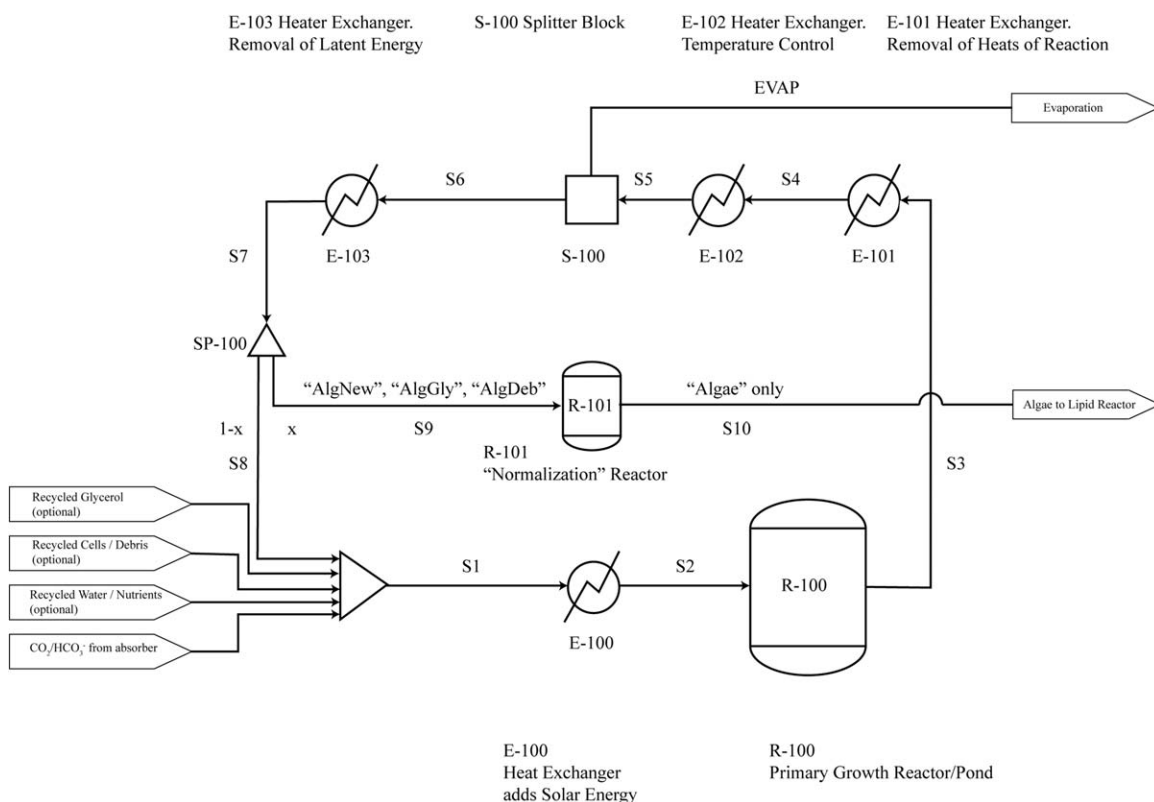


Figure 4. Information recycle loop for algal cell generation.

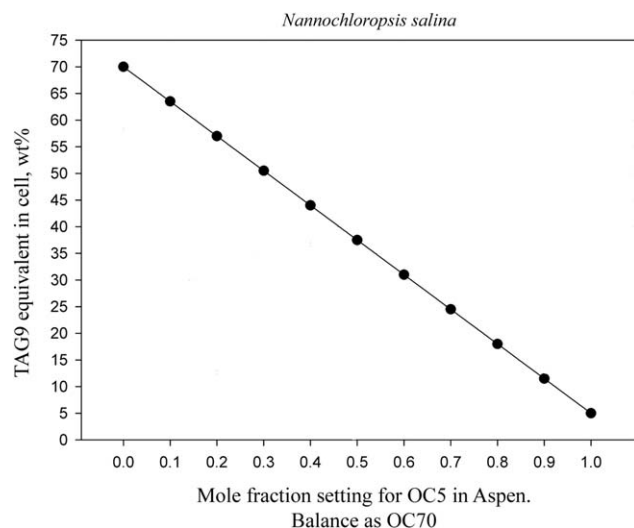


Figure 5. Setting up the simulator to generate oil content between 5 and 70 wt %.

The effluent, S4, with the heats of reaction removed, is sent to a single-stream heat exchanger block, E-102, which cools/heats it to a specified temperature—maintained using utilities. A Calculator block multiplies the specified evaporation flux (Kg/s-m^2) by the pond area to give the isothermal evaporation rate. Then, Separator S-100, removes water in the EVAP stream using a SEP block. A Calculator block computes the heat lost to evaporation and a single-stream heat exchanger block, E-103, adjusts the enthalpy of stream, S6. Finally, the splitter block, SP-100, sends 100x percent of S7 to R-101, a so-called normalization operation (see Identifying the Key Components) to form the Algae species which is sent to the second reaction operation loop. The remaining $100(1 - x)$ percent is recycled to the beginning of the “reaction operation 1 loop.” For the results presented herein, $x = 0.25$. Note that SP-100 simulates the action of a raceway in which the bulk of the algae slurry is recycled. Iterations

about this information recycle loop are repeated until convergence is achieved; that is, until the relative change of the pond area $\frac{|A_1 - A_1^*|}{A_1^*}$ is negligible.

The lipid-production reaction operation is similar to that in Figure 4. While not shown herein, its units are comparable, E-200, R-200, E-201, E-202, S-200, E-203, SP-200, and R-201. Note that the lipid-production reaction operation, modeled with the RSTOIC block in R-200, requires a cultivation area

$$A_2 = \frac{\sum_{i=6}^{13} \xi_i \Delta H_{R_i}}{\Phi_s \phi} \quad (2)$$

It is also important to recognize that both reaction operation models are implemented as small nested iteration loops inside a larger system of recycle loops.

While the entire process simulation flow sheet is not shown herein, its’ recycle loops correspond closely to the recycle streams in Figure 2. Furthermore, the overall material and energy flows through the system are discussed in the section on Analyzing the Model Output.

Algal oil content

In the section on Development of the Key Components for a Model of Algal Biofuel Production, the lipid content of the algal cells was discussed. OC5 was identified as one species created for modeling purposes. While it is not used directly in the case presented herein, it plays a role in the process simulation. For example, if a cell containing 37 wt % oil is desired, it can be modeled either as a mixture of OC35 and OC70 or, alternatively, as a mixture of OC5 and OC70. It was found useful to retain this flexibility as cells containing above or below 35 wt % oil were frequently encountered. Desired oil blends result from formation reactions that occur in parallel and are useful when a specific oil composition is required (Figure 5). It was initially expected that the model would produce cells of a given oil percentage, for example, 45 wt %. The formation of OC35 and OC70 would, therefore, occur in the proportions shown in Figure 5.

Table 6. Energy Logic for the Model

INPUT	CO ₂ supplied	100,000	tonne/year
INPUT	Evaporation rate	3.5	m ³ /hc/h
INPUT	Incoming solar	5.7	kWh/m ² /day
		8.5	GJ/h/hc
INPUT	Useable @ 4% Photosynthetic Efficiency	0.34	GJ/h/hc
Separate cell growth from oil accumulation. Assign to separate ponds (real or imaginary).			
Establish thermodynamics of each macro-reaction			
CALCULATE	Needed by Algae	17.2	GJ/h
CALCULATE	Thus, area required	40.22	hc
CALCULATE	Thus, evaporation required	140.77	m ³ /h
CALCULATE	Latent Heat	2.26	GJ/tonne
CALCULATE	Enthalpy used	317.72	GJ/h
CALCULATE	Incoming energy	343.39	GJ/h
CALCULATE	Heat exchanger E-100 adds solar energy	8.48	GJ/h
Repeat for Oil accumulation			
Loop until converged			
OUTPUT	Area of Pond 1		
OUTPUT	Area of Pond 2		
OUTPUT	Evaporation from each pond		
OUTPUT	Full mass and energy balances		
OUTPUT	Flow in each reactant stream		
OUTPUT	Size of each unit operation		
OUTPUT	Cost of each unit operation		
OUTPUT	Capex & Opex for process		

Table 7. Simulation Results

Process operation	7,884	h/year (90%)
CO ₂ removal	100,000	ton/year CO ₂
Carbon conversion to biodiesel (Methyl Oleate)	94.6	wt%
Biodiesel produced (as Methyl Oleate)	4.5	ton/h
	253,400	barrel oil equivalent/year
Total Area	666.6	hc
Reaction Operation 1 Area for algae generation	90.5	hc
Reaction Operation 2 Area for oil generation	576.0	hc
Oil productivity (based on total area)	16.2	g/m ² /day
Effective oil content	36.5	wt%
Genetic stability requirements —Number of generations/year (binary fision)	41.4	

It was, however, found in practice that the simulator exhausted mass and/or energy before this goal was reached. For clarity in the heuristic model, the reactions were then set to run in series such that OC35 was produced first. Any remaining mass/energy went to the formation of OC70 depending on the simulator's calculations toward a converged mass and energy balance. It took many hundreds of iterations to achieve a converged outcome.

Energy-limited algal growth

This model starts with the assumption that 100,000 tonne per annum of carbon dioxide is available from an industrial source such as a chemical process, cement works, or similar. For the purposes of the model, the source is not important. Based on the previous thermodynamics discussion, the energy required to convert the carbon to algae and algae oil is known. The only source of energy is sunlight, which is determined by location and, therefore, is known. The evaporation rate, which removes substantial quantities of latent energy from the systems, is also known. Thus, the incoming carbon dioxide gives a carbon limitation, whereas the sunlight and evaporation give an energy limitation. This energy logic is displayed in Table 6. It shows that the average evaporation rate at a confidential site studied by the authors is 3.5 m³/(hc·h) and that the average incident solar flux is 5.7 kWh/(m²·day) at the same location.

Note that the calculations above yield the total area of the cultivation pond required. The need for detailed rate constants which are rarely, if ever, available, has been bypassed. Nevertheless, the surface area and all the important energetics and yields are calculated. These results, therefore, correspond to the best achievable case for oil production by solar means for an advanced biofuel from algae.

There is considerable information on the rates of sunlight across the earth, and therefore, the local insolation levels can be fed into the model. In translating the local data into the model, information from Muneer³⁶ was used for rates of daily insolation and its variation over the year for almost any location on earth. It is, therefore, possible to calculate the maximum theoretical yield of either algae or algal oil from a given level of sunlight, as all the energy input comes from the sun. A typical energy input from the sun would be around 20 MJ/m²/day. The calorific value (heat of combustion) of algae is approximately 20 MJ/kg. The maximum output from any algal growth system would be around 1 kg of algae per square meter per day. Algal oil has approxi-

mately twice the calorific value of algae (about 37 MJ/kg). Therefore, for the same amount of incident sunlight, the maximum yield would be about 0.5 kg of algal oil per square meter per day, the upper bound given by the first law of thermodynamics. However, this ideal yield cannot be achieved as it assumes a photosynthetic efficiency of 100%, much higher than typical photosynthetic efficiencies for algae, which is usually between 2 and 5%. To summarize, there are only three factors involved: (1) the solar input, which depends on time and geography; (2) photosynthetic efficiency, which depends on the algal species and conditions; and (3) the calorific value (heat of combustion) of the algae (or the oil), which is not variable.

One missing piece of information remains: pond depth. The required surface area of the bioreactors arises naturally from the energy balance. Depth does not. The model gives the surface area and total biomass by weight. The missing design variable, pond depth, then gives the reactor volume, which in turn determines the cell concentration (g/L) and dilution rate, which at steady state equals the growth rate. It is, therefore, intuitively obvious that depth, cell concentration (dry weight), and growth rate are interlinked. Clearly, the attenuation of light penetration is a key concern. Applying the Lambert–Beer law for the absorption of light through an algal suspension, using a typical molar absorption coefficient ($\epsilon = 7 \text{ m}^2/\text{mol}$ for an apparent molecular weight of 30), the light intensity is attenuated by two orders of magnitude in 0.01 m. Note that pond depths of 0.25 m are typical and were used in this study.

Analyzing the Model Output

The heuristic mode permits analysis of the generalized process block diagram in Figure 2. In this case, Aspen Plus was set to link directly into an Excel spreadsheet to facilitate analysis. Most notably, it permits the identification of problems and possible solutions that can be used to make the system viable at different stages of development—for example, the addition of Calculator Blocks that give results requiring closer monitoring. Similarly, costing and financial modeling which is critical for techno-economic analysis and central to an integrated systems approach to algal biofuel production can be undertaken from the model outputs to ascertain the key drivers for optimizing commercial-scale production. In the development of the model under discussion, 16 areas were analyzed including mass balances, energy balances, effluent streams, bioreactor salinity, energy flows, evaporation, photosynthetic efficiency, glycerol use, carbon flow, water flow, and lost work. They are representative of the types of analysis that are possible using the simulator in a heuristic mode but are not exhaustive. Next, representative results and conclusions derived from the energy-limited algal biofuels model are discussed.

Results

Table 7 summarizes the results after heuristic mode analysis as described herein. The model assumes 90% operation throughout the year (330 day/year), consuming 100,000 tonne of carbon dioxide from flue gas. For Stage One analysis (biodiesel is methyl oleate), carbon conversion to biodiesel is found to be 94.6 wt %, which is 4.5 tonne/h or 253,400 barrels of oil (equivalent). The total surface area is 666.6 hectares, of which 90.5 hectares are associated with

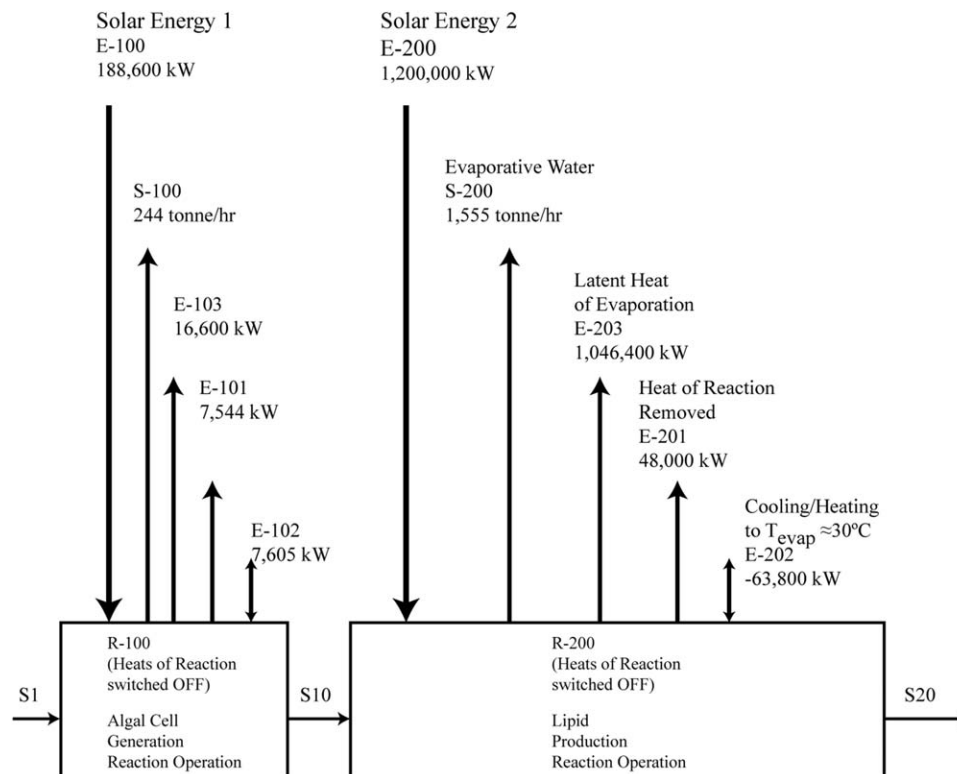


Figure 6. Water evaporation and energy flows to and from reaction operations—calculated using Aspen blocks in Figure 4.

the algae-generating reaction operation and 576 hectares are associated with the second, oil-generating reaction operation. This corresponds to a productivity of oil based on the total active surface area of 16.2 g/m²/day and equivalent to 36.5% w/w oil in the cell. Only small differences have been observed in the preliminary Stage Two analysis using the same approach and this is the subject of ongoing work. Nevertheless, while most actual figures from research and development work are confidential, this is known to be close to observed practice.

In a typical chemical process simulator, a chemical compound is only described by state variables, temperature, pressure, molar composition, and the like. When biological cells are introduced, another variable, the population doubling level,³⁷ is added. It is well known in vaccine production that there are optimal cell generation numbers and these are

meticulously recorded in every laboratory experiment or production batch. As genetic engineering is carried out on algal species, this will also become an issue for biofuels production. In the heuristic model, the cell generation number is calculated at the end of the expected operating period—330 days. It gives the number as the genetic stability requirement the cell must possess, $N(t)/N(0) = 2^n$, where n is the number of generations, assuming binary fission. For the calculations herein, a 10 L inoculum containing 2 g/L of algae is present at $t = 0$. This is equivalent to 0.000002 tonne of algal cells and is $N(0)$. The simulator shows that 57 million tonne of algal cells are produced in 330 days, during which the inoculum has doubled by binary fission³⁸ or other methods. This corresponds to 40 plus cell generations and gives the benchmark against which genetic stability programs (including algae from natural sources), are evaluated. In terms of

Table 8. An Example of Evaporation Rates and their Effect on Temperature

Line							Note
a	Local evaporation rate, (m ³ /m ² /year)	1	2	3	4	5	Determined by location
b	Incoming Solar (GJ/h/hc)	8.5	8.5	8.5	8.5	8.5	Determined by location
c	Useable solar@ 4%	0.34	0.34	0.34	0.34	0.34	4% is around current best case
	Photosynthetic efficiency (GJ/h/hc)						
d	Energy required by algae GJ/h	17.2	17.2	17.2	17.2	17.2	See Figure 4
e	Area required (hc)	50.4	50.4	50.4	50.4	50.4	d/c
f	Pond evaporation rate (m ³ /s)	57.5	115.0	172.4	229.9	287.4	a*e
g	Latent heat of evaporation (GJ/tonne)	2.3	2.3	2.3	2.3	2.3	
h	Heat removed by evaporation (GJ/h)	129.9	259.8	389.7	519.6	649.5	f*g
i	Total Incoming solar (GJ/h)	429.5	429.5	429.5	429.5	429.5	b*e
j	Solar energy remaining in pond (GJ/h)	282.4	152.5	22.6	−107.3	−237.2	i-h-d
k	Liquid velocity (m/s)	0.2	0.2	0.2	0.2	0.2	
l	Volumetric flowrate (m ³ /s)	4.0	4.0	4.0	4.0	4.0	
m	Net temperature rise in pond, ΔT (°C)	4.7	2.5	0.4	−1.8	−3.9	

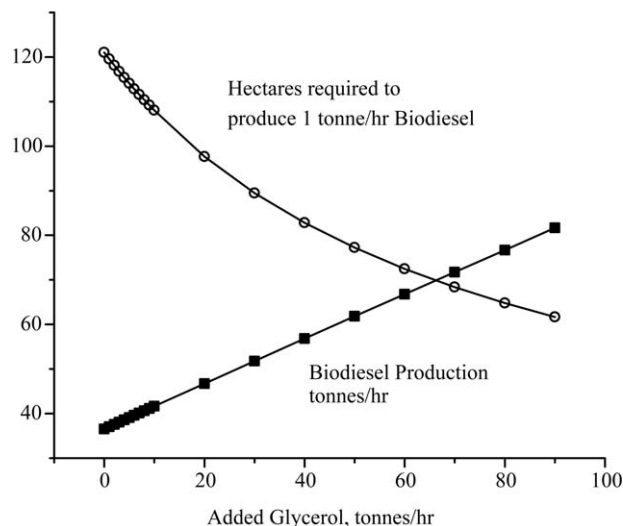


Figure 7. The effect of adding extra glycerol to the process.

genetic stability, this is a high number and the issue of genetic drift must be considered, even for naturally occurring algae cells. Therefore, introducing this biological consideration into the earliest stages of development of a simulation may be helpful and draws attention to this simple, but often overlooked, yet biologically significant calculation.

Energy flows

In the heuristic model, it was useful to turn off the heats of individual reactions to view their effects on the results. This allows the energy flows to be examined more clearly, as shown in Figure 6, which also displays the extents and heats of reaction. These energy flows can be used to assess the relative importance of key factors such as evaporation. There are five flows shown for each reactor in Figure 6. The first is the solar energy influx (E-100/E-200). This gives rise to the evaporation of water (S-100/S-200). The third flow shows the latent heat of evaporation required to make this

happen (E-103/E-203). As the heats of reaction have been switched off in the Aspen block, they need to be explicitly removed (E-101/E-201). Finally, there is an energy flow which may be either cooling or heating of the stream to ensure the desired temperature, usually 30°C, is attained in the reactor for evaporation to occur (E-102/E-202).

Evaporation

In the absence of this integrated systems model, it can be difficult to appreciate the role of evaporation. The undesirable role of evaporation is that it removes water, which is often a scarce resource. A wide range of evaporation rates occur in regions where algal processes are likely to be implemented. It is usually in the range 1–5 m/year which forms the basis of Table 8. Data, of variable quality, are typically available as it is vital to the farming community. The usual unit for reporting is m/year of water equivalent to $\text{m}^3/\text{m}^2/\text{day}$ —with the range of 1–5 examined in line a. Likewise solar insolation is either available or can be calculated with the usual units of reporting $\text{kWh}/\text{m}^2/\text{day}$ with a range of 2–7 being typical. This is held constant here at $5.7 \text{ kWh}/\text{m}^2/\text{day}$ or $8.5 \text{ GJ}/\text{h}/\text{ha}$ for ease of calculation and seen in line b. A very small fraction of the solar power is available for photosynthesis, typically 4% (line c). Aspen, using the iterative information recycle loop in Figure 4, computes $17.2 \text{ GJ}/\text{h}$ required in the reaction operations to grow algal cells—with the reactor area estimated as line d divided by line c. After subtraction of the latent heat of evaporation and the chemical energy requirements of the algae, the residual enthalpy content of the pond is left (line j). Under typical reactor conditions the temperature rise, ΔT , that corresponds to this enthalpy content, can readily be calculated (line m). It can be seen that it takes a local evaporation rate of between 3 and 4 m/year to be thermally neutral. Without additional cooling, the temperature can build to levels that affect the biology.

Glycerol

Glycerol represents an interesting dilemma in terms of the current state of the biofuels market and its place in future

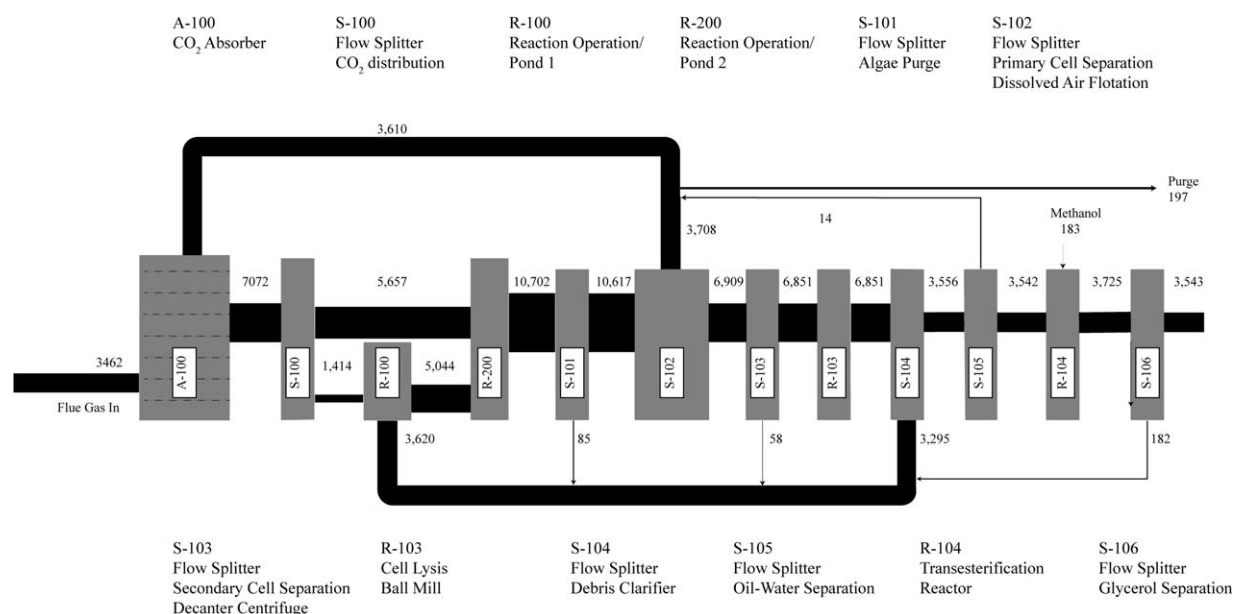


Figure 8. Carbon flow rate (kg/h).

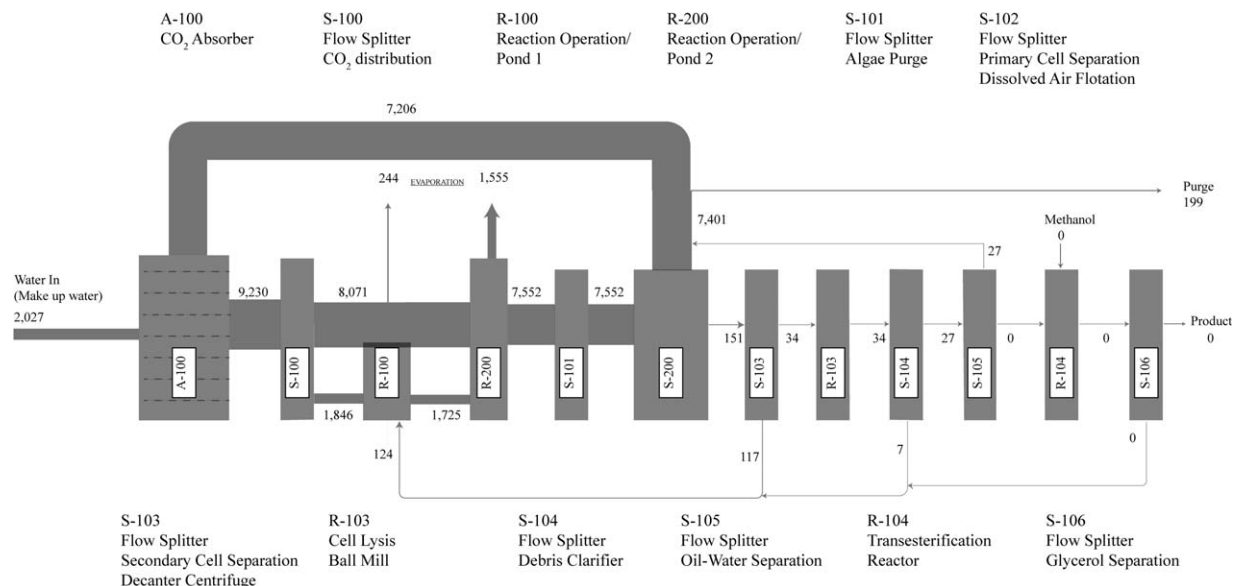


Figure 9. Water flow (tonne/h).

developments in commercial-scale production. Glycerol is an inevitable and major by-product in the manufacture of biodiesel by transesterification. At present, there is a market for glycerol and the process economics benefit from its sale. This market is, at best, limited and would be rapidly overwhelmed if this by-product came from even a modest-sized biodiesel plant. Given an inexpensive source of glycerol, the simulator was used to investigate adding extraglycerol from external sources into the process. Figure 7 shows that while the overall area of the plant clearly increases, glycerol being of lower energy content than biodiesel, the area (hectares) required to produce one unit of biodiesel falls dramatically. This is believed to be an important model output that permits assessment of market shifts over time.

Carbon and water flow

Carbon and water flows are shown in Figures 8 and 9. It is instructive to note the scale of carbon is in kg/h and water flow is in tonne/h, that is, a 1000-fold change in scale. This draws attention to the massive quantities of water that are circulated, which is due to the low concentration of algae in

the process (typically in the range of 0.5–1.0 g/L). Until this is addressed, commercial-scale production will be challenging. The optically dense algal solution means that only the top few centimeters of the pond or bioreactor receive light and, therefore, are biochemically active. Practical solutions to overcome this issue are required, some aspects of which are being addressed in future work.

Lost work

Lost work/exergy calculations, using methods described by Keenan,³⁹ Sussman,⁴⁰ and Seider et al.,⁴¹ are well established. The thermodynamic availability, or exergy, defined as $B = H - T_0S$, where T_0 is a reference temperature taken here at 298.15 K, is calculated for each stream entering and leaving. H and S are estimated by Aspen Plus for each stream. In this case, the sum of inlet stream availabilities is $-7,614,300$ kW and the sum of outlet stream availabilities is $-7,558,600$ kW, giving an availability increase of 55,700 kW. The solar work done on the system in Reaction Operation 1 (187,600 kW) and in Reaction Operation 2 (1,204,000 kW), minus the shaft work needed for compressors and

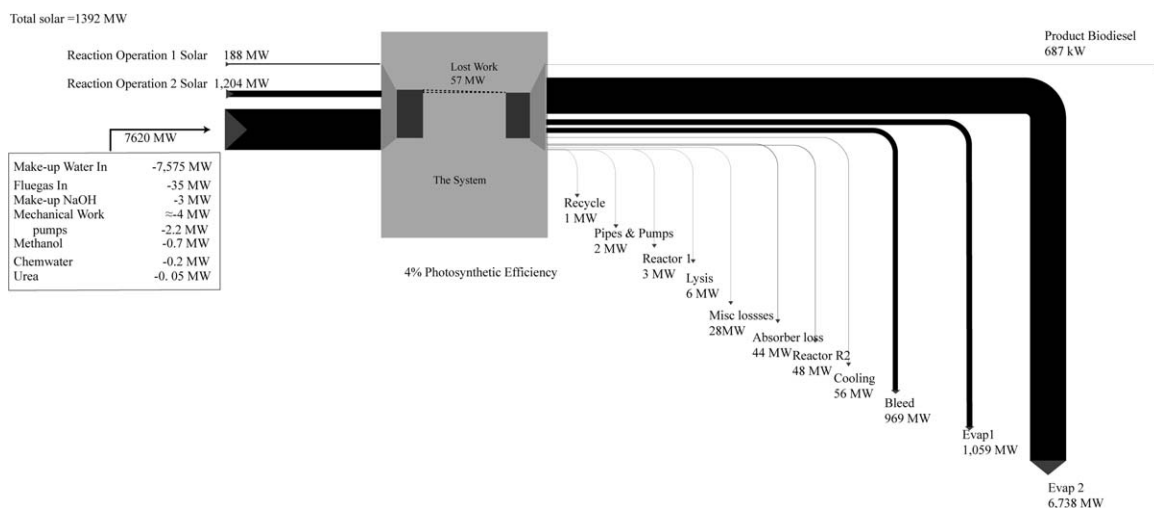


Figure 10. Exergy diagram for lost work analysis.

pumps (3100 kW) yields a net increase of 1,395,000 kW; giving 1,339,000 kW of lost work and a thermodynamic efficiency of just under 4%. Perhaps the most instructive outcome of this analysis is the exergy diagram in Figure 10. Clearly, most of the work is lost in evaporation, and consequently, a very small proportion of sunlight is carried forward in a thermodynamically useful form in the biodiesel. Nevertheless, Figure 10 highlights exciting opportunities for chemical engineers to contribute innovative solutions that reduce lost work, improving sustainability through the development of advanced biofuel production from algae.

Conclusions

The energy-limited model of biofuels production presented herein highlights that an integrated systems approach using computer-aided simulation can be used to find solution to some of the intractable problems of process systems engineering, moving another step toward the commercial-scale production of the next generation of advanced algal biofuels. The development of a process simulator and associated spreadsheet models for the design of processes involving light-driven algal growth for biofuels has been accomplished effectively. Reasonable approximations of the key thermodynamic properties have been made and the energetics of the process established in sufficient detail. It has been shown that the concept of energy (light) limitation is sufficient to bypass the intractable problem of obtaining kinetic data for the postulated chemical reactions. It has also been shown that the simulator can be made to run in discovery (heuristic) mode to predict the missing design information: including the required bioreactor areas, deal with evaporation, and predict likely productivity and oil content of algal cells under likely operating conditions. Reactor depth remains unspecified and is the subject of a parallel study. The required genetic stability also arises naturally from the model. Carbon, water, enthalpy, and exergy flows were examined.

The process simulation and its analysis also highlights three significant issues that need to be addressed if the next generation of algal biofuels is to become commercially viable. First, the results demonstrate that land area requirements are great. Land area, it was shown, can be predicted from the first law of thermodynamics and photosynthetic efficiency. Photosynthetic efficiency can, at least in principle, be improved by genetic engineering and good biochemical control. Establishing good chemical engineering design to operate at appropriate depths for maximum photosynthetic efficiency, while taking due consideration of evaporative effects, remains a critical element for advancing biofuels production to commercial scale. Second, the use of extremely large volumes of water is a major issue. It is clear that while the biofuels process operates at 0.5–1.0 g/L algal biomass, most of the remaining 999–999.5 g/L is water plus salts. Reducing this large volume of water is clearly a future objective. Finally, the impact of recycle cannot be overestimated. While fundamental in optimizing conventional chemical processes, recycle costs, and energy savings have not been fully understood in the algal industry to date. The importance of recycling water, carbon, and debris has been stressed in this model, and the corresponding energetics achieved has been shown. However, it cannot be assumed that the biology will support these recycles. As shown, glycerol recycle has been achieved, but recycling water of high salinity needs to be carefully assessed. Finally, recycling of

debris remains uncertain and laboratory and pilot-plant studies are needed to confirm it as advantageous.

Acknowledgments

The authors would like to acknowledge that this work was prepared, in part, under the auspices of the U.S. Department of Energy under Contract DE-EE0003046 awarded to the National Alliance for Advanced Biofuels and Bioproducts.

Literature Cited

1. Becker EW. *Microalgae, Biotechnology and Microbiology*. Cambridge: Cambridge University Press, 1994.
2. Morimura Y, Nihei T, Sasa T. Outdoor bubbling culture of some unicellular algae. *J Gen Appl Microbiol*. 1955;1(3):173–179.
3. Tamiya H. Mass culture of algae. *Annu Rev Plant Physiol*. 1957;8:309–334.
4. Tamiya H, Hase E, Shabita K, Mituya A, Iwamura T, Nihei T, Sasa T. Kinetics of growth of chlorella, with special reference to its dependence on quality of available light and on temperature. In: Burlew JS, editor. *Algal Culture. From Laboratory to Pilot Plant*. Washington DC: Carnegie Institution of Washington Publication 600, 1953:204–235.
5. von Witsch H, Harder R. Stoffproduktion durch grünalgen und diatomeen in massenkultur. In: Burlew JS, editor. *Algal Culture. From Laboratory to Pilot Plant*. Washington DC: Carnegie Institution of Washington Publication 600, 1953:154–165.
6. Burlew JS. *Algal Culture. From Laboratory to Pilot Plant*. Washington DC: Carnegie Institution of Washington Publication 600, 1953:204–235.
7. Sheehan J, Dunahay T, Benemann J, Roessler P. A look back at the US Department of Energy's Aquatic Species Program: biodiesel from algae. Close-Out Report. National Renewable Energy Laboratory, Golden, CO, 1998. Available at: <http://www.nrel.gov/biomass/pdfs/24190.pdf>. Accessed on December 12, 2012.
8. Bennehan J, Oswald W. Systems and economic analysis of microalgae ponds for conversion of CO₂ to biomass. Final Report. Department of Energy, Pittsburgh Energy Technology Center, Pittsburgh, PA, 1996. Available at: <http://www.osti.gov/bridge/servlets/purl/493389-FXQyZ2/webviewable/493389.pdf>. Accessed on December 12, 2012.
9. U.S. Department of Energy, Office of Energy Efficiency and Renewable Energy, Biomass program. *National Algal Biofuels Technology Roadmap*, 2010. US Department of Energy, Washington DC, Available at: http://www.eere.energy.gov/biomass/pdfs/algal_biofuels_roadmap.pdf. Accessed on December 12, 2012.
10. National Research Council. *Sustainable Development of Algal Biofuels in the United States*. Washington DC: National Academies Press, 2012.
11. Cheng KC, Ogden KL. Algal biofuels: the research. *Chem Eng Prog*. 2011;107:42–47.
12. Anitescu G, Bruno TJ. Liquid biofuels: fluid properties to optimize feedstock selection, processing, refining/blending, storage/transportation, and combustion. *Energy Fuels*. 2012;26:324–348.
13. Wooley RJ, Putsche V. *Development of an ASPEN PLUS Physical Property Database for Biofuels Components*. Golden, CO: NREL/MP, 1996.
14. Quinn J, de Winter L, Bradley T. Microalgae bulk growth model with application to industrial scale systems. *Bioresour Technol*. 2011;102(8):5083–5092.
15. Chisti Y. Biodiesel from microalgae. *Biotechnol Adv*. 2007;25:294–306.
16. Wigmosta MS, Coleman AM, Skaggs RJ, Huesemann MH, Lane LJ. National microalgae biofuel production potential and resource demand. *Water Resour Res*. 2011;47:25.
17. Frank ED, Han J, Palou-Rivera I, Elgowainy A, Wang MQ. *Life-Cycle Analysis of Algal Lipid Fuels with the GREET Model*. Energy Systems Division, Argonne National Laboratory, Lemont, IL, 2011. Available at: <http://greet.es.anl.gov/publication-algal-lipid-fuels>. Accessed on December 12, 2012.
18. Davis R, Aden A, Pienkos PT. Techno-economic analysis of autotrophic microalgae for fuel production. *Appl Energy*. 2011;88:3524–3531.
19. Sun A, Davis R, Starbuck M, Ben-Amotz A, Pate R, Pienkos PT. Comparative cost analysis of algal oil production for biofuels. *Energy*. 2011;36:5169–5179.

20. Weyer KM, Bush DR, Darzins A, Willson BD. Theoretical maximum algal oil production. *Bioenergy Res.* 2010;3:204–213.
21. Dunlop EH, Coaldrake AK. Process and systems for the production of biofuels from algae. Pending US Patent Application. Serial Number 61/676848. Pan Pacific Technologies Pty Ltd, Adelaide, Australia, 2012.
22. Zhang Y, Dub MA, McLean DD, Kates M. Biodiesel production from waste cooking oil: 1. Process design and technological assessment. *Bioresour Technol.* 2003;89:1–16.
23. Zhang Y, Dub MA, McLean DD, Kates M. Biodiesel production from waste cooking oil: 2. Economic assessment and sensitivity analysis. *Bioresour Technol.* 2003;90:229–240.
24. Vyas AP, Verma JL, Subrahmanyam N. A review on FAME production processes. *Fuel.* 2009;89:1–9.
25. Chang A, Liu YA. Integrated process modeling and product design of biodiesel manufacturing. *Ind Eng Chem Res.* 2009;49(3):1197–1213.
26. Pokoo-Aikins G, Nadim A, El-Halwagi MM, Mahalec V. Design and analysis of biodiesel production from algae grown through carbon sequestration. *Clean Technol Environ Policy.* 2010;12:239–254.
27. Barclay B, Weaver C, Metz J. Development of a docosahexaenoic acid production technology using *Schizochytrium*: a historical perspective. In: Cohen Z, Ratledge C, editor. *Single Cell Oils*. Champaign, IL: AOCS Press, 2005:36–52.
28. Sánchez E, Ojeda K, El-Halwagi M, Kafarov V. Biodiesel from microalgae oil production in two sequential esterification/transesterification reactors: pinch analysis of heat integration. *Chem Eng J.* 2011;176–177:211–216.
29. Kemp RB, editor. *Handbook of Thermal Analysis and Calorimetry, Vol. 4. Macromolecules to Man*. Amsterdam: Elsevier, 1999.
30. Bhattacharya A, Motard RL, Dunlop EH. BIOASPEN: system for technology development. NASA Contractor Report. NASA CR-181086, Jet Propulsion Laboratory, Pasadena, 1986.
31. Evans LB. Bioprocess simulation: a new tool for process development. *Nat Biotechnol.* 1988;6:200–203.
32. Wooley R, Ruth M, Glassner D, Sheehan J. Process design and costing of bioethanol technology: a tool for determining the status and direction of research and development. *Biotechnol Prog.* 2008;15:794–803.
33. Galbe M, Zacchi G. Simulation of ethanol production processes based on enzymatic hydrolysis of lignocellulosic materials using Aspen Plus. *Appl Biochem Biotechnol.* 1992;34–35:93–104.
34. O'Grady JP, Morgan JA. Heterotrophic growth and lipid production of *Chlorella protothecoides* on glycerol. *Bioprocess Biosyst Eng.* 2011;34(1):121–125.
35. Cornet J-F, Dussap CG, Gros J-B. Kinetics and energetics of photosynthetic micro-organisms in photobioreactors. *Adv Biochem Eng Biotechnol.* 1998;59:153–224.
36. Muneer T. *Solar Radiation and Daylight Models*, 2nd ed. Amsterdam: Elsevier, 2004.
37. Davis JM. *Basic Cell Culture*, 2nd ed. Oxford: Oxford University Press, 2002.
38. Blackburn S, Parker N. Microalgal life cycles: encystment and excystment. In: Anderson RA, editor. *Algal Culturing Techniques*. Burlington, MA: Elsevier, 2005:399–417.
39. Keenan JH. Availability and irreversibility in thermodynamics. *Br J Appl Phys.* 1951;2:183–192.
40. Sussman MV. *Availability (Exergy) Analysis*. Lexington, MA: Mullen House, 1980.
41. Seider WD, Seader JD, Lewin DR. Second law analysis. Enclosed CD-ROM. In: Seider WD, Seader JD, Lewin DR. *Product and Process Design Principles. Synthesis, Analysis and Evaluation*, 2nd ed. Hoboken, NJ: Wiley, 2004:301–366.

Manuscript received May 2, 2013, and revision received Aug. 19, 2013.